Chiral Amino Acid Recognition by a Porphyrin-Based Artificial Receptor

Yasuhisa Kuroda,* Yusuke Kato, Takuji Higashioji, Jun-ya Hasegawa, Shinichi Kawanami, Masatoshi Takahashi, Nobuyuki Shiraishi, Kazuhito Tanabe, and Hisanobu Ogoshi*

Contribution from the Department of Synthetic Chemistry and Biological Chemistry, Kyoto University, Sakyo-ku, Kyoto 606, Japan

Received April 17, 1995[⊗]

Abstract: Molecular recognition of amino acid methyl esters by doubly bridged porphyrin Zn complexes was investigated. A chiral bridged porphyrin was prepared from the α,α,α,α-atropisomer of *meso*-tetrakis(*o*-aminophenyl)-porphyrin and 4-nitroisophthaloyl chloride. The similar reactions using unsubstituted isophthaloyl, 5-nitroisophthaloyl, and 4,6-dinitroisophthaloyl chlorides as the bridging reagents gave corresponding nonchiral bridged porphyrins. The Zn complex of the chiral porphyrin exhibits significant chiral recognition toward amino acids. For example, the chiral receptor porphyrin shows D-/L-selectivity of 7.5 for valine methyl ester at 293 K in CH_2Cl_2. Comparison of binding behavior of four types of bridged porphyrin Zn complexes and ^1H NMR investigations reveal that the present chiral recognition observed for amino acid methyl esters is caused by favorable hydrogen bond formation between the carbonyl group of the guest and the 3-carboxyamide of the 4-nitroisophthalic bridging benzene. Thermodynamic parameters of the present complexation were also determined, and two types of very strong linear isoequilibrium relationships between the observed entropies and enthalpies were found. One is the linear correlation ($R = 0.993$) between ΔH and $T\Delta S$ values observed for host−guest combinations of bridged porphyrins−amino acid esters, and another is that ($R = 0.997$) observed for combinations of tetraphenylporphyrin−amino acid esters and bridged porphyrins−3-amino-2,4-dimethylpentane. The very large slopes observed for these linear correlations indicate that the significant amount of the conformational freedom of the guests is lost even during the process of simple coordination without hydrogen bond formation.

Introduction

Molecular recognition of amino acids and their derivatives has been one of most attractive objects of host−guest chemistry.[1,2] It is partly due to the importance of amino acids as major components of proteins in natural living systems and partly due to their potential characteristics which make amino acids suitable for guest molecules in artificial recognition systems. One of these characteristics of amino acids is their versatile ability to form complexes with other molecules via various types of interaction modes which cover almost all kinds of intermolecular interactions ever found in the chemistry of molecular recognition.[2,3] Amino and carboxyl groups in amino acids are expected

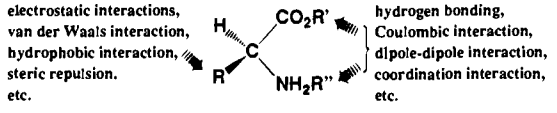

to act as binding sites for hydrogen bonding and electrostatic interactions such as Coulombic and dipole−dipole interactions. Residual groups on the α-carbon can also form additional recognition sites, where not only electrostatic interactions but also other types of interactions such as van der Waals or hydrophobic interactions and/or even steric repulsion may

* To whom correspondence should be addressed.

[⊗] Abstract published in *Advance ACS Abstracts*, October 15, 1995.

(1) For recent reviews on molecular recognition, see: (a) Cram, D. J. *Angew. Chem., Int. Ed. Engl.* **1988**, *27*, 1009. (b) *Frontiers in Supramolecular Organic Chemistry and Photochemistry*; Schneider, H-J., Dürr, H., Eds.; VHC: Weinheim, 1990. (c) Vögtle, F. *Supramolecular Chemistry, an Introduction*; John Wiley & Sons: New York, 1991. (d) Molecular Recognition (Tetrahedron Symposia No. 56). Hamilton, A. D., Ed.; *Tetrahedron* **1995**, *51*.

(2) For recognition of cation forms of amino acids, see: (a) Lehn, J.-M.; Sirlin, C. *J. Chem. Soc., Chem. Commun.* **1978**, 949. (b) Peacock, S. C.; Domeier, L. A.; Gaeta, F. C. A.; Helgeson, R. C.; Timko, J. M.; Cram, D. J. *J. Am. Chem. Soc.* **1978**, *100*, 8190. (c) Sogah, G. D. Y.; Cram, D. J. *J. Am. Chem. Soc.* **1979**, *101*, 3035. (d) Newcomb, M.; Toner, J. L.; Helgeson, R. C.; Cram, D. J. *J. Am. Chem. Soc.* **1979**, *101*, 4971. (e) Peacock, S. S.; Walba, D. M.; Gaeta, F. C. A.; Helgeson, R. C.; Cram, D. J. *J. Am. Chem. Soc.* **1980**, *102*, 2043. (f) Davidson, R. B.; Bradshaw, J. S.; Jones, B. A.; Dalley, N. K.; Christensen, J. J.; Izatt, R. M.; Morin, F. G.; Grant, D. M. *J. Org. Chem.* **1984**, *49*, 353. (g) Naemura, K.; Fukunaga, R.; Yamanaka, M. *J. Chem. Soc., Chem. Commun.* **1985**, 1560. (h) Murakami, Y.; Ohno, T.; Hayashida, O.; Hisaeda, Y. *J. Chem. Soc., Chem. Commun.* **1991**, 950. For carboxylate anion form, see: (i) Behr, J.-P.; Lehn, J.-M. *J. Am. Chem. Soc.* **1973**, *95*, 6108. (j) Pirkle, W. H.; House, D. W.; Finn, J. M. *J. Chromatogr.* **1980**, *192*, 143. (k) Tsukube, H. *Tetrahedron Lett.* **1981**, *22*, 3981. (l) Echavarren, A.; Galán, A.; Lehn, J.-M.; de Mendoza, J. *J. Am. Chem. Soc.* **1989**, *111*, 4994. (m) Konishi, K.; Yahara, K.; Toshishige, H.; Aida, T.; Inoue, S. *J. Am. Chem. Soc.* **1994**, *116*, 1337. For recognition of twitterionic forms of amino acids, see: (n) Sunamoto, J.; Iwamoto, K.; Mohri, Y.; Kominato, T. *J. Am. Chem. Soc.* **1982**, *104*, 5502. (o) Rebek, J., Jr.; Askew, B.; Nemeth, D.; Parris, K. *J. Am. Chem. Soc.* **1987**, *109*, 2432. (p) Galán, A.; Andreu, D.; Echavarren, A. M.; Prados, P.; de Mendoza, J. *J. Am. Chem. Soc.* **1992**, *114*, 1511. For recognition of neutral amide and peptide form, see: (q) Dobashi, A.; Hara, S. *Tetrahedron Lett.* **1983**, *24*, 1509. (r) Spisni, A.; Corradini, R.; Marchelli, R.; Dossena, A. *J. Org. Chem.* **1989**, *54*, 684. (s) Liu, R.; Sanderson, P. E. J.; Still, W. C. *J. Org. Chem.* **1990**, *55*, 5184. (t) Yoon, S. S.; Still, W. C. *J. Am. Chem. Soc.* **1993**, *115*, 823. (u) Borchardt, A.; Still, W. C. *J. Am. Chem. Soc.* **1994**, *116*, 7467. For neutral cyclic peptide form, see: (v) Famulok, M.; Jeong, K.-S.; Deslongchamps, G.; Rebek, J., Jr. *Angew. Chem., Int. Ed. Engl.* **1991**, *30*, 858. (w) Jeong, K. S.; Tjivikua, T.; Muehldorf, A.; Deslongchamps, G.; Famulok, M.; Rebek, J., Jr. *J. Am. Chem. Soc.* **1991**, *113*, 201. (x) Cristofaro, M. F.; Chamberlin, A. R. *J. Am. Chem. Soc.* **1994**, *116*, 5089. For recognition of neutral ester forms of amino acids, see: (y) Rebek, J., Jr.; Askew, B.; Ballester, P.; Doa, M. *J. Am. Chem. Soc.* **1987**, *109*, 4119. (z) Pirkle, W. H.; Pochapsky, T. C. *J. Am. Chem. Soc.* **1987**, *109*, 5975.

(3) Greenstein, J. P.; Winitz, M. *Chemistry of Amino Acids*; Krieger Publishing Co.: Malabar, FL, 1984.

0002-7863/95/1517-10950$09.00/0

operate according to the chemical and physical properties of the residual groups. If the host−guest system contains a metal ion, one can also expect coordination interactions between the amino acid and the host system. Thus, host−guest pairs containing amino acids may provide an ideal chemical tool, by which we can systematically examine functions and roles of intermolecular interactions operating in recognition systems, especially multipoint recognition ones.

Of the various types of amino acid receptors, the authors have been particularly interested in construction of artificial receptors based on porphyrin frameworks.[4] Porphyrins are very attractive molecules as a "platform" for molecular recognition from the synthetic chemistry viewpoint.[4,5] The relatively rigid and flat structure of porphyrin is sometimes suitable as the framework for artificial receptors which are required to recognize spatial shapes of guest organic molecules. Furthermore, it is possible to attach various types of functional groups at four meso positions and eight β-positions of pyrroles of porphyrin. A variety of synthetic methods for functionalizing porphyrins at these positions has been developed.[6] Such flexibility of design and synthesis makes porphyrin an attractive platform for molecular recognition. It should be also noted that unique spectroscopic characteristics of porphyrins in NMR, ESR, UV−visible, and emission spectra make it easy to detect and characterize molecular recognition between host and guest molecules.[6]

Recently, we reported a new type of amino acid recognition system which was designed on the basis of a tetraphenylporphyrin framework.[7] The host molecules used in this work are doubly bridged tetraphenylporphyrin derivatives of which chiral binding sites are easily constructed on the porphyrin planes by employing unsymmetric bridging reagents. The Zn complexes of these porphyrins show the significant chiral recognition ability in complexation with various types of amino acid esters. The main attractive interactions between the host and guest molecules are coordination of the amino group on the Zn metal and hydrogen bonding between the carbonyl group of the amino acid and the amide NH group of the host. The third element for recognition which is necessary for chiral recognition is provided from a steric interaction between the host and the residual group of the amino acid. This simultaneous recognition of amino and carbonyl functionalities of amino acids via attractive interactions is in contrast to amino acid recognition by chiral crown ether in which the amino group is recognized by attractive hydrogen bonding but the carbonyl group acts as a simple steric element for recognition.[2b-d]

In this paper, we report the details of molecular recognition of amino acids with the doubly bridged porphyrin.

Scheme 1

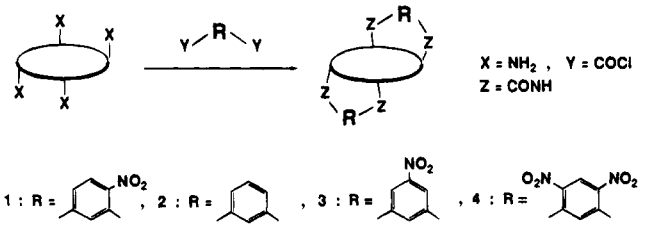

Results and Discussion

Preparation of Doubly Bridged Porphyrins. The doubly bridged porphyrins were first synthesized by Collman et al. as oxygen binding models using α,α,α,α-atropisomer of *meso*-tetrakis(*o*-aminophenyl)porphyrin and unsubstituted- and 5-nitroisophthaloyl chloride as the bridging reagent.[8] The similar reaction for α,α,β,β-atropisomer is expected to give another type of doubly bridged porphyrins as shown in Scheme 1. Especially when an unsymmetrically substituted bridging reagent such as 4-nitroisophthaloyl chloride is employed, the reaction may afford the interesting doubly bridged porphyrin, **1**, which consists of meso and chiral isomers (Figure 1). This type of chiral porphyrins has a C_2 symmetry, which provides identical chiral spaces on both sides of the porphyrin plane. In the actual experiment, the bridging reaction of the porphyrin with the diacid chloride was carried out in THF to give a 1:1 mixture of the corresponding meso and chiral porphyrins, which are easily separated by usual silica gel chromatography. The chiral porphyrin was further resolved into the enantiomers on the chiral HPLC column (Figure 2a). These enantiomeric porphyrins show symmetric Cotton effects toward each other at their Soret bands in circular dichroism spectra as shown in Figure 2b. Since the absolute configurations of these chiral porphyrins are not yet determined, the enantiomers were tentatively classified as **1**(+) and **1**(−) according to the sign of the observed Cotton effect at the Soret region.

Three other porphyrins having symmetric bridging isophthaloyl moieties, **2**, **3**, and **4**, were also prepared as reference compounds by a similar method. Slight modification, however, was necessary for the preparation of **3** and **4**, i.e., the reactions of the porphyrin with 5-nitro- or 4,6-dinitroisophthaloyl chloride in THF gave no appreciable amount of these doubly bridged porphyrins, while the desired products were obtained from the reaction using *N*-methyl-2-pyrrolidone as the solvent.[9] The low yield of the reaction in THF may be due to low solubility of the singly bridged intermediate porphyrins in this solvent. The structures of these porphyrins were determined by ^{1}H NMR, FAB mass, elemental analysis, and electronic spectra.

Amino Acid Recognition. The host molecules for amino acid recognition used in this work were Zn complexes of these porphyrins which were prepared by the usual method using zinc acetate. Association constants between the porphyrin Zn complexes and amino acid methyl esters were determined by UV−visible spectroscopic titration. In the first experiments, we used chloroform containing 0.5% ethanol as a stabilizer as the solvent for titration. The typical binding constants thus obtained are summarized in Table 1.

In order to obtain further information, we determined thermodynamic parameters for present amino acid recognition in the same solvent. Using van't Hoff plot of association

(4) (a) Aoyama, Y.; Asakawa, M.; Yamagishi, A.; Toi, H.; Ogoshi, H. *J. Am. Chem. Soc.* **1990**, *112*, 3145. (b) Ogoshi, H.; Hatakeyama, H.; Yamamura, K.; Kuroda, Y. *Chem. Lett.* **1990**, 51. (c) Ogoshi, H.; Hatakeyama, H.; Kotani, J.; Kawashima, A.; Kuroda, Y. *J. Am. Chem. Soc.* **1991**, *113*, 8181. (d) Kuroda, Y.; Hatakeyama, H.; Inakoshi, N.; Ogoshi, H. *Tetrahedron Lett.* **1993**, *34*, 8285. (e) Mizutani, T.; Ema, T.; Yoshida, T.; Kuroda, Y.; Ogoshi, H. *Inorg. Chem.* **1993**, *32*, 2072. (f) Kuroda, Y.; Hatakeyama, H.; Seshimo, H.; Ogoshi, H. *Supramol. Chem.* **1994**, *3*, 267. (g) Mizutani, T.; Ema, T.; Tomita, T.; Kuroda, Y.; Ogoshi, H. *J. Am. Chem. Soc.* **1994**, *116*, 4240.

(5) (a) Hamilton, A.; Lehn, J.-M.; Sessler, J. L. *J. Am. Chem. Soc.* **1986**, *108*, 5158. (b) Lindsey, J. S.; Kearney, P. C.; Duff, R. J.; Tjivikua, P. T.; Rebek, J. *J. Am. Chem. Soc.* **1988**, *110*, 6575. (c) Salehi, A.; Mei, H.-Y.; Bruice, T. C. *Tetrahedron Lett.* **1991**, *32*, 3453. (d) Harriman, A.; Kubo, Y.; Sessler, J. L. *J. Am. Chem. Soc.* **1992**, *114*, 388. (e) Kuroda, Y.; Ogoshi, H. *Synlett* **1994**, 319.

(6) *Porphyrins and Metalloporphyrins*; Smith, K. M., Ed.; Elsevier Scientific Publishing: New York, 1975.

(7) Kuroda, Y.; Kato, Y.; Higashioji, T.; Ogoshi, H. *Angew. Chem., Int. Ed. Engl.* **1993**, *32*, 723.

(8) (a) Collman, J. P.; Gagne, R. R.; Reed, C. A.; Halbert, T. R.; Lang, G.; Robinson, W. T. *J. Am. Chem. Soc.* **1975**, *97*, 1427. (b) Collman, J. P.; Brauman, J. I.; Fitzgerald, J. P.; Hampton, P. D.; Naruta, Y.; Michida, T. *Bull. Chem. Soc. Jpn.* **1988**, *61*, 47.

(9) Korshak, V. V.; Rusanov, A. L.; Plieva, L. K.; Kereselidze, M. K.; Lekae, T. V. *Macromolecules* **1976**, *9*, 626.

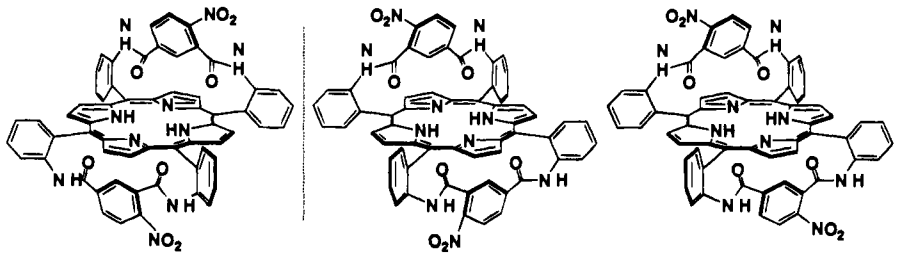

1(±) meso-1

Figure 1. Structures of chiral and meso porphyrins doubly bridged by 4-nitroisophthaloyl groups.

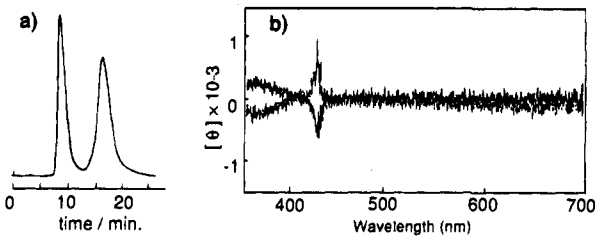

Figure 2. (a) Chiral separation of 1(±) on HPLC. The separation conditions are as follows: column, CHIRALCEL OD (0.46 × 25 cm); eluent, hexane/EtOH = 1:1 (1 mL/min); detection at 428 nm. (b) Circular dichroism spectra of optically pure enantiomers of 1(+) and 1(−) in THF.

Table 1. Binding Constants (K_a) at 293 K for Porphyrin 1(−)·Zn and 1(+)·Zn−Amino Acid Methyl ester Complexation in $CHCl_3$[a]

	K_a (M^{-1})[a]	
amino acid ester	1(−)·Zn	1(+)·Zn
L-Val-OMe	$(2.4 \pm 0.1) \times 10^4$	$(4.9 \pm 0.3) \times 10^3$
L-Leu-OMe	$(1.7 \pm 0.1) \times 10^4$ [b]	$(4.2 \pm 0.2) \times 10^3$
L-Phe-OMe	$(2.0 \pm 0.1) \times 10^4$	$(4.1 \pm 0.2) \times 10^3$
L-phenylglycine-OMe	$(1.3 \pm 0.1) \times 10^4$	$(3.8 \pm 0.4) \times 10^3$
L-DOPA-OMe[c]	$(2.4 \pm 0.1) \times 10^4$	$(5.4 \pm 0.5) \times 10^3$
D-DOPA-OMe[c]	$(6.0 \pm 0.5) \times 10^3$	$(2.2 \pm 0.2) \times 10^4$

[a] The data were obtained in $CHCl_3$ containing ethanol as a stabilizer (see the text for details). [b] At 293.5 K. [c] At 288 K.

constants collected at 276−313 K give a good straight line to afford the necessary thermodynamic parameters, but the ΔS values thus evaluated were unexpectedly small and slightly positive, i.e., for example, the ΔH and ΔS values for complex formation between 1(−)·Zn and L-valine methyl ester are −5.1 kcal/mol and +2.5 eu, respectively. Since relatively large entropy losses are usually expected for the present types of complex formation,[10] we re-examined possible equilibrium processes for the present recognition other than simple bimolecular complex formation. One of the most plausible candidates for such possibility is solvent participation in the equilibrium process, and therefore, we investigated the effect of ethanol contained in spectroscopic grade $CHCl_3$ used in this work. When ethanol-free $CHCl_3$ is used as the solvent, 1(−)·Zn shows the Soret absorption band at 428 nm, which shifted to 433 nm on addition of ethanol as shown in Figure 3. Benesi−Hildebrand-type analysis for titration data gives 50 ± 1 M^{-1} as the binding constant of ethanol at 293 K in $CHCl_3$. Thus, it is clear that the present amino acid recognition system is competitively inhibited by ethanol binding. For example, the titration experiment using ethanol-free $CHCl_3$ reveals that the association constant between 1(−)·Zn and L-valine methyl ester $(8 \pm 1) \times 10^5$ M^{-1}, which is over 30 times larger than that in

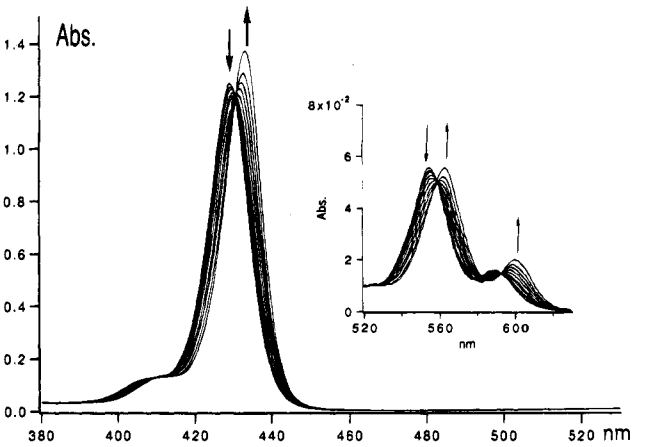

Figure 3. UV−vis titration of 1(−)·Zn with ethanol at 293 K in $CHCl_3$: [1(−)·Zn] = 4.81×10^{-6}; [ethanol] = 0, 1.1, 2.2, 4.4, 6.5, 11, 17, 25, 41, and 72×10^{-3} M.

$CHCl_3$ containing ethanol (Table 1).[11] We also found that more stable and alcohol-free CH_2Cl_2 gives essentially same results as those in ethanol-free $CHCl_3$. The typical titration experiment data for 1(−)·Zn and L-valine methyl ester in CH_2Cl_2 are shown in Figure 4. The original Soret band at 428 nm shifts to 437 nm, and clear isosbestic points are observed at 433, 562, 586, and 595 nm. The result indicates formation of a 1:1 complex between this host−guest pair, and usual curve fitting analysis for observed absorbance changes gives the association constants to be $(8.2 \pm 1.0) \times 10^5$ M^{-1} at 293 K. Thus, we decided to re-evaluate all data by using alcohol-free CH_2Cl_2. The association constants thus determined are shown in Table 2. Inspection of Table 2 shows that the receptor 1(−)·Zn binds L-valine methyl ester 89 times more strongly than the corresponding amine, 3-amino-2,4-dimethylpentane (DMPA), which suggests that the present recognition contains not only coordination of the amino group on Zn but also hydrogen bonding between the carboxymethyl group of the guest and the amide NH of the host. In contrast, 1(+)·Zn shows weak affinity even toward the same amino acid, though its association constants are still larger than those of TPP·Zn. Thus, the present chiral porphyrin exhibits significant chiral recognition toward amino acids. For example, the association constants of 1(−)·Zn and 1(+)·Zn for L-valine methyl ester are 8.2×10^5 and 1.1×10^5 M^{-1}, respectively, which correspond to D/L-selectivity of 7.5 for valine methyl ester at 293 K in CH_2Cl_2. It should be also noted that

(10) (a) Page, M. I.; Jencks, W. P. *Proc. Natl. Acad. Sci. U.S.A.* **1971**, *68*, 1678. (b) Simanek, E. E.; Mammen, M.; Gordon, D. M.; Chin, D.; Mathias, J. P.; Seto, C. T.; Whitesides, G. M. *Tetrahedron* **1995**, *51*, 607.

(11) The ΔH and ΔS values for complex formation of 1(−)·Zn with L-valine methyl ester and ethanol in pure $CHCl_3$ are −22.8 ± 2.3 kcal/mol, −50 ± 8 eu, −7.0 ± 0.7 kcal/mol and −16 ± 2 eu, respectively. The results indicate that ca. one-third of the enthalpy and entropy changes for amino acid recognition in ethanol-free $CHCl_3$ may be compensated by those of the ligand exchange process in $CHCl_3$ containing ethanol. The observed enthalpy and entropy changes (−5.1 kcal/mol, 2.5 eu) for amino acid recognition in $CHCl_3$ containing ethanol show that further compensation may occur by desolvation processes of ethanol around the host and/or guest molecules.

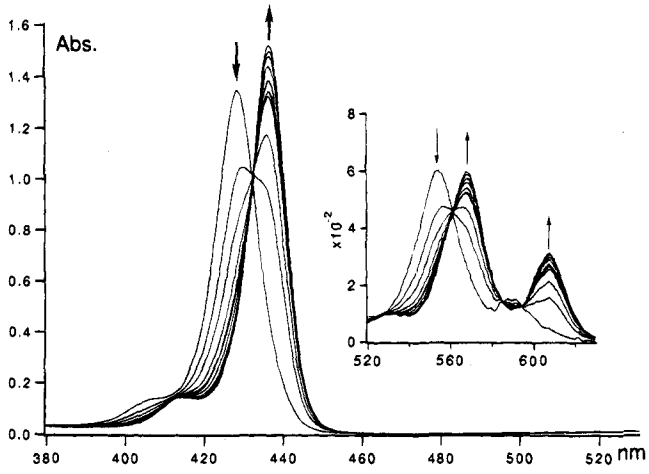

Figure 4. UV−vis titration of 1(−)·Zn with L-valine methyl ester at 293 K in CH_2Cl_2: [1(−)·Zn] = 5.10 × 10^{-6}; [L-Val-OMe] 0, 2.5, 5.0, 6.0, 7.5, 9.9, 15, 24, 37, and 56 × 10^{-6} M.

the present chiral porphyrin receptor shows meaningful D/L-selectivity of 4.1 even for the smallest chiral amino acid, alanine.[12]

NMR Studies on Amino Acid Recognition. In order to clarify the structure of the present amino acid−**1**(−)·Zn complex, NMR spectra of the complex were investigated. The spectra of **1**(−)·Zn in the presence of different concentrations of L-valine methyl ester are shown in Figure 5. In this example, over 96% of used **1**(−)·Zn is expected to exist as a complex with the guest under the conditions shown in Figure 5d. Although we could not assign the signals observed for H_a/H_b, H_c/H_d, $H_e/H_f/H_k/H_l$, and $H_g/H_h/H_i/H_j$ to each proton uniquely (see the inset of Figure 5 for the notation of these protons), the spectrum of the aromatic region obtained in the absence of the guest shows a clear C_2 symmetric structure of **1**(−)·Zn in which each proton signal appears in pairs as shown in Figure 5a. In the presence of an excess amount of the guest, these C_2 symmetric characters are maintained because of rapid ligand exchange between identical front and back binding sides of **1**(−)·Zn but signal separation becomes clear as shown in Figure 5d. In contrast with relatively small changes of chemical shifts for these aromatic protons, two amide protons show large downfield shifts from 6.76 and 7.34 ppm to 7.45 and 7.65 ppm on addition of the guest. The observation strongly indicates hydrogen bonding interactions between these amide protons and the carbonyl group of the guest.[13]

The ^{1}H NMR data also give interesting information on the structure of the guest in the complexing form. The spectra of the higher field region for the mixture of L-valine methyl ester and **1**(−)·Zn are shown in Figure 6. Under the conditions shown Figure 6, over 99% of the guest is evaluated to form the complex with **1**(−)·Zn and, as expected, significant upfield shifts due to the strong shielding effect of the porphyrin were observed for all proton signals of the guest. The chemical shifts of free and complexing L-valine methyl ester are summarized in Table 3.

Among these, the amino protons of the guest showed an extraordinarily large upfield shift due to direct coordination onto the central Zn atom of the porphyrin.[4] Furthermore, the proton on the α-carbon of L-valine methyl ester was also found to exhibit a similar amount of upfield shift upon complexation. This observation strongly indicates that the α-proton of the amino acid ester is located in close contact with the porphyrin plane. The isopropyl group is also estimated to be located in the shielding area of the porphyrin, as judged by appreciable amounts of upfield shifts observed for their protons resonances. Interestingly, methoxy protons showed the smallest upfield shift, which may suggest a more off-centered location of this methyl group on the porphyrin compared with those of other groups.

Effect of a Nitro Group for Molecular Recognition. As mentioned in the previous section, the present chiral porphyrin **1** has chiral recognition ability toward amino acid methyl esters. Since chiral recognition logically requires at least spatially oriented three-point interactions between the host and the guest, the observed chiral recognition indicates that there is a significant difference between the hydrogen-bonding abilities of two amide groups at the 1- and 3-positions of the bridging benzene ring of **1**(−)·Zn and **1**(+)·Zn. In order to clarify the origin of such different hydrogen-bonding abilities, the recognition behavior of reference bridged porphyrins, **2**, **3**, and **4**, was investigated. The binding constants between zinc complexes of these porphyrins and amino acid methyl esters at 293 K are also summarized in Table 2. Although the hydrogen-bonding abilities of four amide groups in **2**, **3**, and **4** are expected to be identical and, therefore, they show no chiral recognition for amino acid derivatives, comparison of the observed binding constants evidently indicates that the nitro group on the bridged benzene ring plays an important and essential role in present molecular recognition. For example, the ability of **2**·Zn to bind L-valine methyl ester is over 21 times weaker than that of **1**(−)·Zn. Even **3**·Zn having 5-nitroisophthaloyl bridges shows only 1/12 of the binding constant of **1**(−)·Zn for the guest. These observations suggest that the hydrogen-bonding ability of the amide NH at the ortho position of the nitro group is largely enhanced by the electronic effect of the nitro group. The conclusion is also supported by the observation that the dinitro bridged receptor **4**·Zn shows practically the same magnitude of the binding constant as that of **1**(−)·Zn. The result is reasonable because only one hydrogen-bonding interaction is operating in the present amino acid recognition. This situation contrasts with that observed for the trench porphyrin system in which all four amide groups are used as hydrogen-bonding sites for tartrates, and therefore, bridging with 4,6-dinitroisophthalic acid results in a dramatic enhancement of the binding ability.[14] The electronic effect of the nitro group in the isophthalic systems may be estimated from the pK_a values of these acids. The pK_a values of some isophthalic acid derivatives are shown in Figure 7.[15] The data show that the 3-carboxylic acid of 4-nitroisophthalic acid is $10^{1.76}$ (~58) and $10^{0.92}$ (~8.3) times stronger acid than those of unsubstituted and 5-nitroisophthalic acids, respectively. It should be noted that the 3-carboxylic acid of 4-nitroisophthalic acid is a $10^{1.12}$ times stronger acid even compared to the 1-carboxylic acid of the same compound. The hydrogen-bonding abilities of the amide NH's of **1**(−)·Zn are reasonably considered to be affected by such a unsymmetrical electronic effect of the nitro group on their proton-donating character. Thus, it is concluded that the present chiral recognition observed for amino acid methyl esters is caused by favorable hydrogen bond formation between the carbonyl group of the guest and the 3-carboxyamide of the 4-nitroisophthalic bridging benzene. From these considerations, we can now draw

(12) The D-/L-selectivities are temperature dependent. This trend is striking especially for the recognition system which shows large entropy difference for D-/L-recognition (see Table 4). For example, very large D-/L-selectivity of over 40 is actually observed for phenylalanine recognition at 264 K.

(13) Jeffrey, G. A.; Saenger, W. *Hydrogen Bonding in Biological Structures*; Springer-Verlag: New York, 1991.

(14) Kuroda, Y.; Kato, Y.; Ito, M.; Hasegawa, J.; Ogoshi, H. *J. Am. Chem. Soc.* **1994**, *116*, 10338.

(15) (a) Wegsheider, R. *Monatsh. Chem.* **1916**, *37*, 219. (b) Wegsheider, R. *J. Chem. Soc.* **1916**, *110*, 467. (c) Venimadhavan, S.; Shelly, K. P.; Stewart, R. *J. Org. Chem.* **1989**, *54*, 2483.

Table 2. Binding Constants (K_a) at 293 K for Porphyrin Receptors−Amino Acid Methyl Ester Complexation in CH_2Cl_2

	K_a (M^{-1})[a]					
guest	**1**(−)·Zn	**1**(+)·Zn	TPP·Zn	**2**·Zn	**3**·Zn	**4**·Zn
L-Val-OMe	$(8.2 \pm 1.0) \times 10^5$	$(1.1 \pm 0.1) \times 10^5$	$(9.5 \pm 0.4) \times 10^3$	$(3.8 \pm 0.2) \times 10^4$	$(6.9 \pm 0.2) \times 10^4$	$(6.6 \pm 0.4) \times 10^5$
L-Leu-OMe	$(7.5 \pm 0.6) \times 10^5$	$(8.6 \pm 0.5) \times 10^4$ [b]	$(8.1 \pm 0.3) \times 10^3$	$(2.8 \pm 0.1) \times 10^4$	$(6.7 \pm 0.1) \times 10^4$	$(5.9 \pm 0.3) \times 10^5$
L-Phe-OMe	$(5.0 \pm 0.1) \times 10^5$ [b]	$(7.1 \pm 0.4) \times 10^4$ [b]	$(1.1 \pm 0.1) \times 10^4$	$(2.6 \pm 0.1) \times 10^4$	$(6.8 \pm 0.2) \times 10^4$	$(4.4 \pm 0.1) \times 10^5$
L-Ala-OMe	$(1.8 \pm 0.1) \times 10^5$ [b]	$(4.4 \pm 0.2) \times 10^4$ [b]	$(5.0 \pm 0.3) \times 10^3$	$(1.7 \pm 0.1) \times 10^4$	$(3.1 \pm 0.1) \times 10^4$	$(1.9 \pm 0.1) \times 10^5$
L-PheG-OMe[c]	$(2.0 \pm 0.1) \times 10^5$	$(1.6 \pm 0.2) \times 10^5$	$(6.5 \pm 0.3) \times 10^3$	$(2.7 \pm 0.1) \times 10^4$	$(5.7 \pm 0.2) \times 10^4$	$(3.8 \pm 0.1) \times 10^5$
DMPA	$(9.2 \pm 0.3) \times 10^3$ [d]		$(7.8 \pm 0.6) \times 10^3$			

[a] Standard deviations are given in parentheses. [b] At 293.5 K. [c] Phenylglycine. [d] The association constant for *meso*-**1**·Zn.

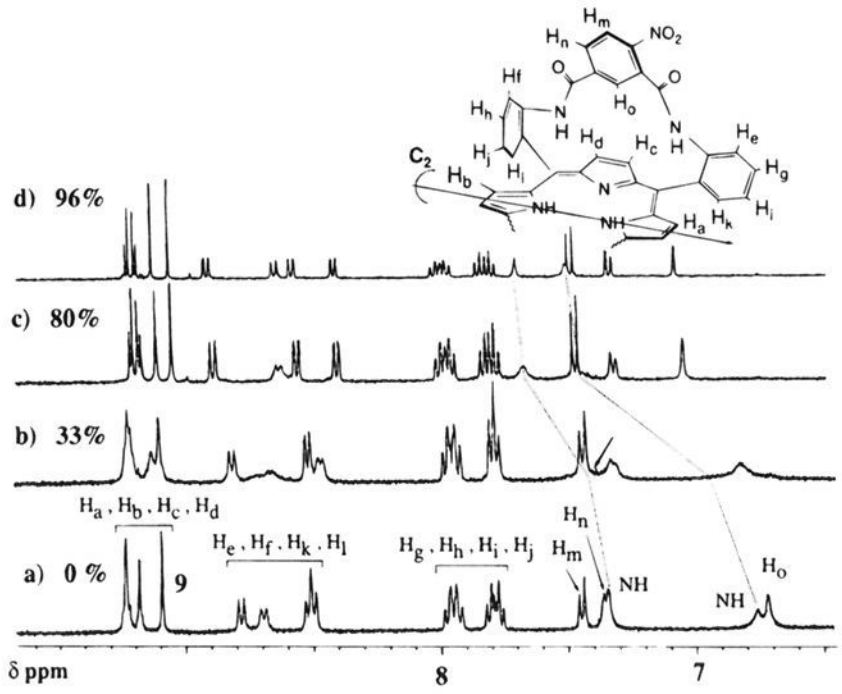

Figure 5. ^{1}H NMR spectra of free and complexing **1**(−)·Zn at 297 K in CD_2Cl_2. The inset shows the notation of the host's protons. The spectra of [**1**(−)·Zn] = 1.0×10^{-3} M were recorded in the presence of (a) none, (b) 3.4×10^{-4} M, (c) 9.4×10^{-4} M, and (d) 2.0×10^{-3} M of L-Val-OMe, respectively. The percent numbers show the ratios of complex formation of **1**(−)·Zn which are estimated from the association constant. The downfield shift of NH protons is indicated by the dashed line.

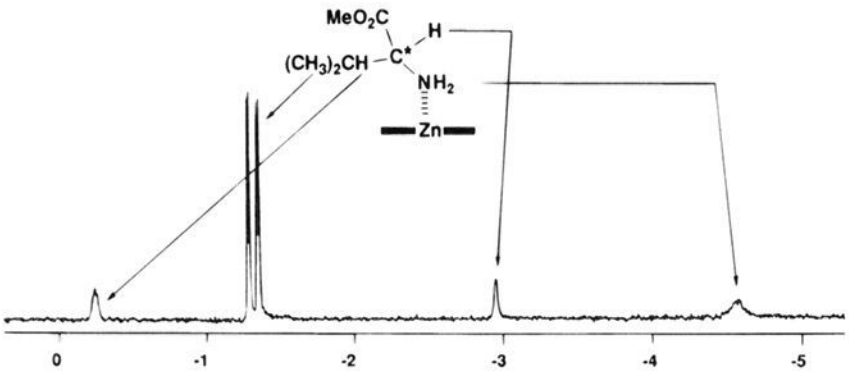

Figure 6. ^{1}H NMR spectrum of complexing L-Val-OMe at 297 K in CD_2Cl_2: [**1**(−)·Zn] = 9.1×10^{-4} M; [L-Val-OMe] = 3.5×10^{-4} M.

Table 3. ^{1}H NMR Chemical Shifts of Free and Complexing L-Valine Methyl Ester[a]

protons in L-Val-OMe	δ_{free} (ppm)	$\delta_{complex}$ (ppm)	$\Delta\delta$ = $\delta_{complex} - \delta_{free}$ (ppm)
NH_2	1.47	−4.57	−6.04
OCH_3	3.75	2.80	−0.95
C^*H^b	3.31	−2.90	−6.21
$(CH_3)_2CH$	2.03	−0.22	−2.25
$(CH_3)_2$	0.97	−1.24	−2.21
	0.89	−1.33	−2.22

[a] Complex with **1**(−)·Zn in CD_2Cl_2 at 301 K. [b] The proton on the α-carbon.

an absolute structure of the **1**(−)·Zn−guest complex as shown in Figure 8 assuming L-configuration of the amino acid. The model also shows general agreement with results obtained from ^{1}H NMR experiments: close contact of the proton on the

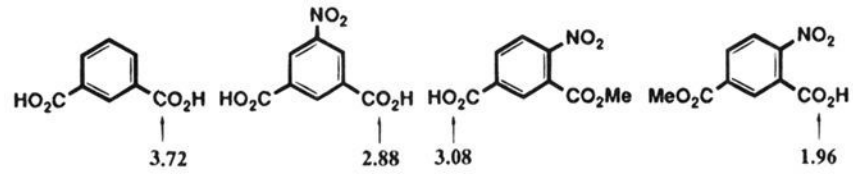

Figure 7. Acid dissociation constants for isophthalic acid derivatives.

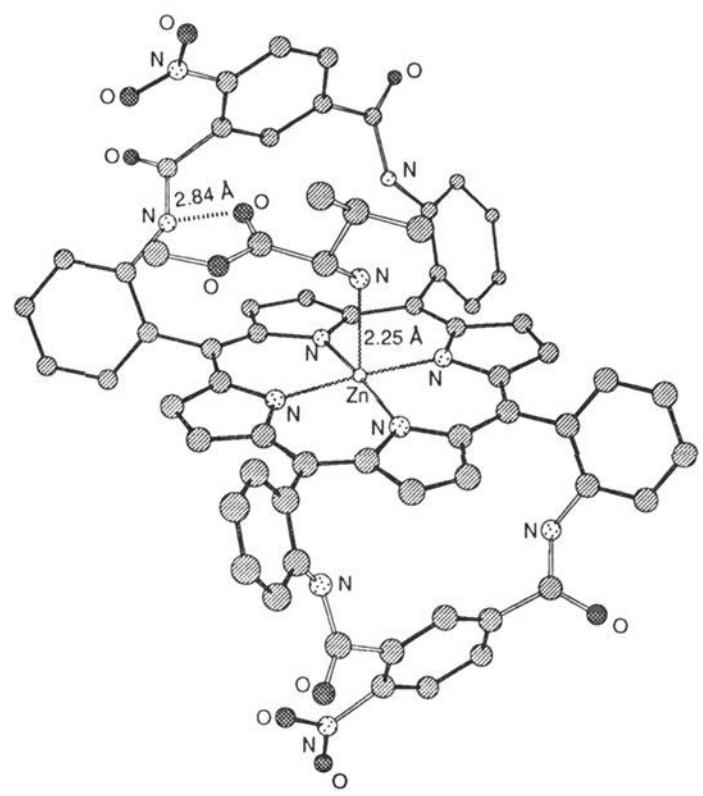

Figure 8. Proposed structure of the L-valine methyl ester−**1**(−)·Zn complex. The geometry was optimized by the PM3 method.[26] All protons are omitted, and heteroatoms are labeled for clarity. In this geometry, the distance between the carbonyl oxygen of the guest and the amide nitrogen of the host is 2.84 Å and the amide proton (not shown) locates within 1.9 Å from the carbonyl oxygen. Other characteristic distances are also evaluated as follows: the Zn−N coordination distances = 3.15 Å, and the distance between, the α-proton of the guest and the averaged porphyrin plane = 3.10 Å.

α-carbon to the porphyrin plane and rather off-centered location of the methoxy group.

Thermodynamic Parameters for Amino Acid Recognition. It has been well recognized that thermodynamic data for equilibrium processes sometimes give further insight into their detailed mechanisms.[16] Since the present amino acid recognition systems may provide an example of systematic analyses of molecular recognition, we attempted to determine thermodynamic parameters for complexation between amino acid derivatives and receptor porphyrins, zinc complexes of **1**(−), **1**(+), **2**, **3**, **4**, and TPP. van't Hoff-type analyses of association constants collected at 277−303 K gave the ΔH and ΔS values summarized in Table 4.

In the present case, no serious deviation from the simple van't Hoff relationship due to heat capacity changes was observed

(16) (a) Leffler, J. E.; Grunwald, E. *Rates and Equilibria of Organic Reactions*; Dover Publications, Inc.: New York, 1963. (b) Hine, J. *Structural Effects on Equilibria in Organic Chemistry*; John Wiley & Sons: New York, 1975.

Table 4. Thermodynamic Parameters for Complex Formation between Various Types of Porphyrin Zn Complexes and Amino Acid Esters

run	host	guest	$-\Delta H$ (kcal/mol)	ΔS (cal/mol K)
1	**1**(−)·Zn	L-Val-OMe	22.5 ± 3.7	−50 ± 13
2		L-Phe-OMe	23.2 ± 2.2	−53 ± 8
3		L-Ala-OMe	17.2 ± 0.4	−35 ± 2
4		L-Leu-OMe	19.6 ± 1.0	−40 ± 4
5		L-PheG-OMe[a]	22.1 ± 0.9	−51 ± 4
6		DMPA[b]	10.7 ± 0.4	−18 ± 2
7	**1**(+)·Zn	L-Val-OMe	16.2 ± 0.7	−32 ± 3
8		L-Phe-OMe	12.1 ± 0.4	−19 ± 2
9		L-Ala-OMe	13.8 ± 0.3	−26 ± 1
10		L-Leu-OMe	13.8 ± 0.5	−25 ± 2
11		L-PheG-OMe[a]	9.4 ± 1.0	−8 ± 4
12	**2**·Zn	L-Val-OMe	13.1 ± 0.3	−24 ± 2
13		L-Phe-OMe	12.8 ± 0.2	−23 ± 1
14		L-Ala-OMe	11.5 ± 0.3	−20 ± 1
15		L-Leu-OMe	12.8 ± 0.3	−23 ± 2
16		L-PheG-OMe[a]	12.2 ± 0.3	−21 ± 2
17		DMPA[b]	10.1 ± 0.8	−16 ± 3
18	**3**·Zn	L-Val-OMe	16.2 ± 0.4	−33 ± 2
19		L-Phe-OMe	12.8 ± 0.3	−21 ± 1
20		L-Ala-OMe	12.7 ± 0.3	−23 ± 1
21		L-Leu-OMe	14.8 ± 0.4	−28 ± 2
22		L-PheG-OMe[a]	13.7 ± 0.3	−25 ± 1
23		DMPA[b]	7.3 ± 0.3	−7 ± 1
24	**4**·Zn	L-Val-OMe	21.5 ± 2.0	−46 ± 7
25		L-Phe-OMe	18.4 ± 0.8	−37 ± 3
26		L-Ala-OMe	14.7 ± 0.3	−26 ± 1
27		L-Leu-OMe	19.0 ± 0.9	−38 ± 3
28		L-PheG-OMe[a]	19.6 ± 0.9	−41 ± 3
29		DMPA[b]	9.8 ± 0.5	−16 ± 2
30	TPP·Zn	L-Val-OMe	13.9 ± 0.3	−29 ± 2
31		L-Phe-OMe	12.5 ± 0.3	−24 ± 2
32		L-Ala-OMe	11.3 ± 0.4	−22 ± 2
33		L-Leu-OMe	13.6 ± 0.4	−28 ± 2
34		L-PheG-OMe[a]	9.2 ± 0.9	−14 ± 4
35		DMPA[b]	11.5 ± 0.4	−21 ± 2

[a] L-Phenylglycine methyl ester. [b] 3-Amino-2,4-dimethylpentane.

within the present temperature range.[17] It is evident by the data in Table 4 that, as the present complex formation becomes more exothermic, the process becomes entropically less favorable and the entire recognition processes were driven enthalpically. The data suggest a strong correlation between the complexation enthalpy and entropy.[18] We found two types of very strong linear relationships between the observed entropies and enthalpies. One is the linear correlation (R = 0.993) between ΔH and $T\Delta S$ values observed for host−guest combinations of bridged porphyrins−amino acid esters (Figure 9a), and another is that (R = 0.997) observed for combinations of tetraphenylporphyrin (TPP)−amino acid esters and bridged porphyrins−DMPA (Figure 9b). It should be noted that this classification clearly corresponds with the difference of interaction modes expected for these two host−guest combinations, i.e., the former equilibrium is expected to be driven by simultaneous coordination and hydrogen bond interactions but there is no hydrogen bonding site in the latter.

One of the interesting proposals for such isoequilibrium relationships is expressed by eq 1, which yields eq 2 upon integration.[19] It was concluded that the slope, α, and intercept, $T\Delta S_0$, of eq 2 provided good indexes to the conformational

$$T\Delta(\Delta S) = \alpha\Delta(\Delta H) \quad (1)$$

$$T\Delta S = \alpha\Delta H + T\Delta S_0 \quad (2)$$

changes during complex formation and the extent of desolvation, respectively. From the present data sets, a slope of α = 0.86 and an intercept of 4.5 kcal mol^{-1} for the data in Figure 9a and those of α = 0.99 and 5.1 kcal mol^{-1} for the data in Figure 9b were obtained, respectively. These large slopes which are close to unity indicate that significant conformational change may accompany the processes of both complex formations.[19] The results contrast with previous findings reported for receptor porphyrins, where the small slope of α = 0.60 for the porphyrin−quinone system[20] and that of α = 0.61 for the metalloporphyrin−pyridine or picoline system[21] indicated the minimal conformational changes of the hosts upon complexation.[22] Since the frameworks of these receptor porphyrins are generally considered to be rigid, the observed discrepancies must be due to the different characteristics of the guest molecules. Thus, the differences between the slopes of the present and previous data suggest that the flexible amino acids undergo significantly larger conformational changes during the present complex formation than do rigid pyridine or picoline derivatives. The very large slope observed for the TPP−amino acid esters and bridged porphyrins−DMPA systems indicates that a significant amount of the conformational freedom of the guests is lost even during the process of simple coordination without hydrogen bond formation. Space-filling molecular models indicate that internal rotations of the amino acid methyl esters on porphyrins are indeed restricted significantly by steric repulsion between the residual groups of the guest and the porphyrin plane and/or *meso*-phenyl groups of the hosts. The slope of α = 0.86 observed for the bridged porphyrins−amino acid ester system suggests that further conformational restrictions are added on hydrogen bond formation between the host−guest pairs. Assuming that the ΔH and ΔS values for the TPP−amino acid system essentially reflect the thermodynamic contribution of simple coordination of the amino acids on porphyrin, these conformational restrictions due to hydrogen bond formation may be evaluated by subtracting these thermodynamic quantities from those for corresponding bridged porphyrin−amino acid systems.[4g,23] The result is shown in Figure 10, in which the difference entropies, $T\Delta(\Delta S)$ ($T(\Delta S_{\text{bridged porphyrin−amino acid}} - \Delta S_{\text{TPP−amino acid}})$, are plotted against the corresponding $\Delta(\Delta H)$. The resulting slope and intercept are α = 0.88 and 1.1 kcal mol^{-1} (R = 0.992), respectively. This slope indicates that further significant conformational restriction may indeed occur on hydrogen bond formation, though the entropy loss due to this process seems to be less compensatory against the enthalpy gain compared with that of the coordination process (α = 0.99). The intercept values of these plots also show another interesting

(17) (a) Smithrud, D. B.; Wyman, T. B.; Diederich, F. *J. Am. Chem. Soc.* **1991**, *113*, 5420. (b) Stauffer, D. A.; Bassans, R. E.; Dougherty, D. A. *J. Org. Chem.* **1990**, *55*, 2762. (c) Zhu, C. Y.; Bradshaw, J. S.; Oscarson, J. L.; Izatt, R. M. *J. Inclusion Phenom.* **1992**, *12*, 275.

(18) (a) Glew, D. N.; Robertson, R. E. *J. Phys. Chem.* **1956**, *60*, 332. (b) Wassermann, A. *J. Chem. Soc.* **1942**, 621. (c) Lumry, R.; Rajender, S. *Biopolymers* **1970**, *9*, 1125. (d) Bennetto, H. P.; Caldin, E. F. *J. Chem. Soc. A* **1971**, 2198. (e) Ueoka, R.; Matsumoto, Y. *J. Org. Chem.* **1984**, *49*, 3774.

(19) (a) Inoue, Y.; Hakushi, T. *J. Chem. Soc., Perkin Trans. 2* **1985**, 935. (b) Inoue, Y.; Amano, F.; Okada, N.; Inada, H.; Ouchi, M.; Tai, A.; Hakushi, T.; Liu, Y.; Tong, L.-H. *J. Chem. Soc., Perkin Trans. 2* **1990**, 1239. (c) Inoue, Y.; Hakushi, T.; Liu, Y.; Tong, L.-H.; Shen, B.-J.; Jin, D.-S. *J. Am. Chem. Soc.* **1993**, *115*, 475. (d) Macartney, D. H.; Waddling. C. A. *Inorg. Chem.* **1994**, *33*, 5912.

(20) Aoyama, Y.; Asakawa, M.; Matsui, Y.; Ogoshi, H. *J. Am. Chem. Soc.* **1991**, *113*, 6233.

(21) (a) Kadish, K. M.; Schaeper, D. *J. Chem. Soc., Chem. Commun.* **1980**, 1273. (b) Vogel, G. C.; Stahlbush, J. R. *Inorg. Chem.* **1977**, *16*, 950. (c) Cole, S. J.; Curthoys, G. C.; Magnusson, E. A.; Phillips, J. N. *Inorg. Chem.* **1972**, *11*, 1024. (d) Miller, J. R.; Gorough, G. D. *J. Am. Chem. Soc.* **1952**, *74*, 3977. (e) Walker, F. A.; Benson, M. J. *J. Am. Chem. Soc.* **1980**, *102*, 5530. (f) Cole, S. J.; Curthoys, G. C.; Magnusson, E. A. *J. Am. Chem. Soc.* **1970**, *92*, 2991.

(22) Inoue, Y.; Liu, Y.; Tong, L.-H.; Shen, B.-J.; Jin, D.-S. *J. Am. Chem. Soc.* **1993**, *115*, 10637.

(23) (a) Wells, T. N. C.; Fersht, A. R. *Biochemistry* **1986**, *25*, 1881. (b) Ho, C. K.; Ferst, A. R. *Biochemistry* **1986**, *25*, 1891.

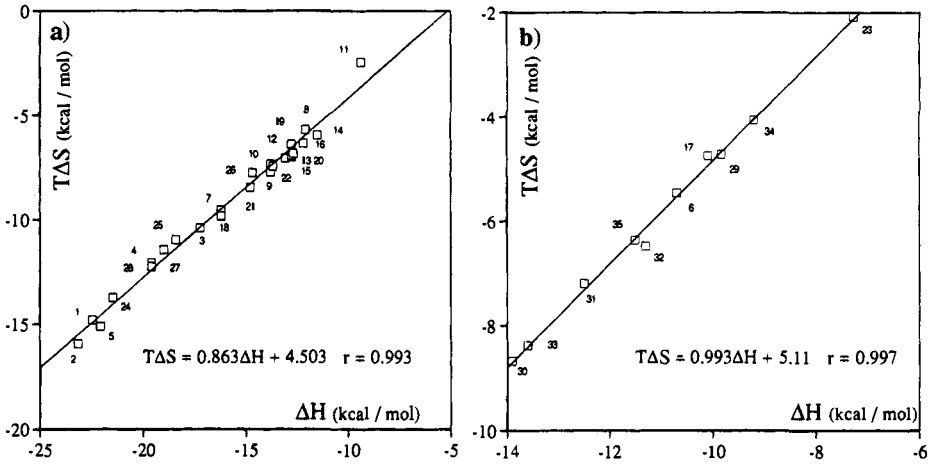

Figure 9. Enthalpy–entropy compensation plot for (a) complexation of the bridged porphyrins, **1**(±), **2**, **3**, and **4**, with amino acid esters and (b) complexation of the bridged porphyrins with DMPA and TPP with amino acid esters. All data were taken from Table 4, and the $T\Delta S$ terms were evaluated at T = 298 K. The linear relationship and correlation coefficient calculated by the least squares method are shown in the figure. The numbers in the graph refer to the entries shown in Table 4.

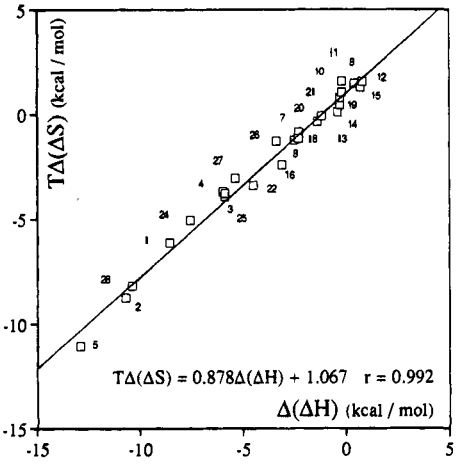

Figure 10. Enthalpy–entropy compensation plot for the hydrogen-bonding contribution in amino acid recognition (see the text for details). The linear relationship and correlation coefficient calculated by the least squares method are shown in the figure. The numbers in the graph refer to the corresponding entries in Table 4 which are used for the calculation.

aspect of the present molecular recognition. According to the classification of Inoue et al., the intercept of 5.1 kcal mol^{-1} shown in Figure 9b indicates that the coordination equilibrium is significantly affected by solvent participation (desolvation).[19] It should be noted that simple ligand exchange may not correspond with this solvent participation as discussed in the previous section. As expected, the (hypothetical) process of intramolecular hydrogen bond formation is accompanied with less extensive desolvation, as indicated by the small intercept of 1.1 kcal mol^{-1} evaluated from Figure 10. Although, at the present stage, we cannot discuss the detailed mechanism of observed desolvation during the coordination equilibrium, the solvent cohesive interaction which is expected to be weak but still exist for CH_2Cl_2 is an interesting candidate for the mechanism of the present solvent participation.[24]

Conclusions

Among various attempts to utilize porphyrins as the platform for molecular recognition, the present doubly bridged porphyrins provide an unique class of artificial receptors. This class of molecules is especially effective as a porphyrin receptor which has its recognition site on the porphyrin plane. To design this type of receptor, one can use various types of substituted tetraphenylporphyrin atropisomers as the basic porphyrin skelton and a wide range of difunctionalized molecules, even such as cyclodextrin, as the bridging reagent.[25] Such flexibility of design make it possible to prepare a variety of artificial receptors systematically. This work demonstrates that chirality can be introduced into the porphyrin receptor simply by using the unsymmetric bridging reagent and its affinity for the amino acid may also be tuned easily by slight modification of the bridging benzene. The thermodynamic analysis of present molecular recognition reveals significant conformational change of the guest molecule during complex formation, which had not been observed for the previous recognition system consisting of porphyrin receptors and rigid guests. The conformational restriction of the guest seems to be significant even for the process of the single point coordination on the present TPP delivatives. Although addition of the second interaction, hydrogen bonding, results in further additional conformational restriction of the guest, the effect may be less compensatory against the enthalpy gain. In other words, the enthalpy gained from the second attractive interaction contributes more effectively to the total stabilization ($-\Delta G$) of the complex.

Experimental Section

General Remarks. ^{1}H NMR spectra were recorded on a JEOL FX-90Q (90 MHz), a JEOL GX-400 (400 MHz), or a JEOL α-500 (500 MHz). ^{1}H NMR chemical shifts are referenced to internal $CDCl_3$ (^{1}H δ 7.25 ppm) relative to Me_4Si at 0 ppm. Data are reported as follows: chemical shift, multiplicity (s = singlet, d = doublet, t = triplet, q = quartet, m = multiplet, b = broad), coupling constant (hertz), and relative intensities. Electronic absorption spectra were performed on a Hitachi U-3410 spectrometer, multichannel photodiode array spectrometer Hewlett-Packard HP-8452A, thermostated at given temperatures with a circulation system, NESLAB Instruments, Inc. RTE-9. Circular dichroism spectra were performed on a JASCO J-600. Mass spectra were obtained with a JEOL JMS DX-300 or a JEOL JMS-SX102A mass spectrometer. HPLC experiments were performed on a TOSOH HLC-837 or Waters M600E equipped with a TOSOH UV-8010 variable-wavelength detector and Waters M991 photodiode array detector. Details of the titration procedures were reported previously.[4e]

Solvents. Tetrahydrofuran (THF) was distilled over sodium benzophenone ketyl. *N*-Methyl-2-pyrrolidone (NMP) was distilled over

(24) Smithrud, D. B.; Diederich, F. *J. Am. Chem. Soc.* **1990**, *112*, 339.

(25) (a) Kuroda, Y.; Hiroshige, T.; Sera, T.; Shiroiwa, Y.; Tanaka, H.; Ogoshi, H. *J. Am. Chem. Soc.* **1989**, *111*, 1912. (b) Kuroda, Y.; Egawa, Y.; Seshimo, H.; Ogoshi, H. *Chem. Lett.* **1994**, 2361.

(26) Stewart, J. J. P. MOPAC Version 6.0. *QCPE Bull.* **1989**, *9*, 10.

calcium hydride. Pyridine was distilled over potassium hydroxide. Lutidine (2, 6-) was distilled just before use. Deuterated chloroform for the ^{1}H NMR measurements was 99.96% deuterated grade purchased from Nacalai Tesque, Inc., and purified as follows: basic alumina (~3 mL) and 4A molecular sieves were dried by warming with "heat gun" in vacuo for 10 min, the activated alumina was transferred to a short column made by a disposable pipet, and $CDCl_3$ was passed through the column. The first fraction (~1 mL) should be discarded in the case of the NMR measurements at a very low concentration of porphyrin because of contamination with small but nonnegligible amounts of impurities. The next fraction was stored with the molecular sieves for overnight. Deuterated dichloromethane was stored with the activated 4A molecular sieves to remove water before use. Dichloromethane used for UV−vis titration was specially prepared reagent grade for spectroscopy purchased from Nacalai Tesque, Inc., and employed without further purification. Anhydrous chloroform for UV measurements was prepared by washing with water (to remove EtOH), drying with anhydrous magnesium sulfate, and distilling over phosphorus pentoxide. Anhydrous chloroform (without EtOH) was stored in the dark to avoid photochemical formation of phosgene and used within 2 days. Chloroform stabilized with ethanol was DOTITE Spectrosol containing about 0.5% of ethanol purchased from Dojindo Laboratories.

Materials. Dicarboxylic acid chlorides of 4-nitroisophthalic, 5-nitroisophthalic, and 4,6-dinitroisophthalic acids were prepared as reported in the literature.[27]

All amino acid methyl ester hydrochloride used was purchased from Nacalai Tesque, Inc., except L-phenylglycine methyl ester, which was prepared by introducing dry hydrogen chloride gas into a suspension of the free amino acid in absolute methanol.[28] After neutralization with 15 mL of saturated $NaHCO_3$(aq) and extraction with dichloromethane, all amino acid esters were freshly distilled (L-Val-OMe, 70 °C, 8 mmHg; L-Leu-OMe, 100 °C, 3 mmHg; L-Phe-OMe, 125 °C, 1 mmHg; L-Ala-OMe, 60 °C, 10 mmHg; L-phenylglycine-OMe, 130 °C, 2 mmHg) just before use. The reference guest, 3-amino-2,4-dimethylpentane, was purchased from Janssen Chimica and distilled (35 °C, 20 mmHg) before use. α,α,β,β-Tetrakis(*o*-aminophenyl)porphyrin (α,α,β,β-T_{am}PP) was prepared as reported in the literature.[8] Other commercially available chemicals were purchased from Wako Pure Chemical Industries, Ltd., Nacalai Tesque, Inc., or Tokyo Kasei Kogyo Co., Ltd., and employed without further purification, unless stated otherwise. Analytical thin-layer chromatography was performed with pre-coated Merck silica gel 60, F254 (0.2 mm layers on glass plates). Column chromatography was performed using Merck Kieselgel 60.

Synthesis. Preparation of Chiral Porphyrin 1. To a THF solution (400 mL) of pyridine (0.95 mL) in a 1-L round-bottomed flask equipped with two dropping funnels were slowly added a solution of 4-nitroisophthaloyl chloride (1.47 g, 5.92 mmol) in THF (100 mL) and a solution of α,α,β,β-TamPP (0.50 g, 0.74 mmol) in THF (100 mL), respectively, in 2 h at room temperature. After additional stirring at ambient temperature (2 h), concentrated aqueous Na_2CO_3 was added until the green solution turned deep purple. The organic phase was washed with brine, dried with Na_2SO_4, filtered, and evaporated in vacuo using a rotary evaporator. The residue was dissolved in DMF (~50 mL), and silica gel powder (~30 mL) was added to the solution.

The solvent was slowly concentrated to dryness under reduced pressure, and the resultant adsorbent was loaded onto a silica gel column (Ø 4.5 × 27 cm, $CHCl_3$), eluting with THF. The single purple band was collected and reduced to a small volume using a rotary evaporator. Hexane was added to the THF solution, and a purple powder was precipitated, filtered, washed with hexane, and concentrated to dryness (0.1 mmHg, room temperature, 2 h) to give the mixture of diastereomeric **1** (meso and racemic), yield 0.47 g (0.46 mmol, 62%). The diastereomers (meso and racemic) were separated on the preparative HPLC silica gel column (YMC SH-043-5 (Ø 2.0 × 25 cm), benzene/Et_2O (9/1 v/v)) to give pure meso and racemic **1** in the ratio 1:1.

Resolution of the antipodes of racemic **1** was carried out by using a chiral HPLC column (Daicel Chiralcel OD (Ø 2.0 × 25 cm), hexane/EtOH/diethylamine (1:1:0.15 v/v/v)). The HPLC operation was carried out under the condition of 7.0 mL/min of flow rate at room temperature and monitoring at 428 nm. The mixture of **1**(+) and **1**(−) was dissolved in THF and subjected to HPLC, and two peaks, **1**(+) at 9.8 min and **1**(−) at 20.0 min, were collected. The separation factor α and the resolution factor R_s were 2.98 and 1.98, respectively. UV−vis of **1**(±) (DMF) λ_{max}, nm (log ε): 429 (5.42), 526 (4.09), 559 (3.50), 598 (3.56), 655 (3.49). CD spectrum of **1**(±) in THF (236−700 nm): 5.1×10^4 (424 nm), -2.5×10^4 (360 nm), 5.9×10^3 (292 nm), -1.8×10^4 (254 nm). CD of **1**(−): -5.1×10^4 (424 nm), 2.5×10^4 (360 nm), -5.9×10^3 (292 nm), 1.8×10^4 (254 nm). ^{1}H NMR of **1**(±) (400 MHz, $CDCl_3$−CF_3CO_2D): δ 9.55 (s, 2H, pyrrole), 9.31 (s, 2H, pyrrole), 9.21 (s, 2H, pyrrole), 9.25 (s, 2H, pyrrole), 8.57 (d, J = 7.9 Hz, 2H), 8.54 (d, J = 7.9 Hz, 2H), 8.39 (d, J = 7.9 Hz, 2H), 8.04 (d, J = 7.9 Hz, 2H), 8.14 (dd, J = 7.9, 7.9 Hz, 4H), 8.07 (dd, J = 7.9, 7.9 Hz, 2H), 8.00 (dd, J = 7.9, 7.9 Hz, 2H), 7.44 (d, J = 8.0 Hz, 2H, bridged benzene), 7.02 (d, J = 8.0 Hz, 2H, bridged benzene), 6.09 (bs, 2H, bridged benzene). FABMS of **1**(±):*m/z* 1025 (MH^+).

Preparation of 1(±)·Zn. To a THF solution (30 mL) of a mixture of *meso*-**1** and **1**(±) (26.1 mg, 25.5 μmol) and 2,6-lutidine (~6 mL) was added saturated methanolic $Zn(OAc)_2$ (~8 mL), and the mixture was refluxed for 1 h. The metal insertion was checked by monitoring the vis spectrum of an aliquot of the THF solution. After being cooled to room temperature, the reaction mixture was loaded on a silica gel column (Ø 2.8 × 10 cm) and the column was eluted with THF. The red-purple fraction was collected and evaporated under reduced pressure. The residue was dissolved in CH_2Cl_2 (100 mL) and washed with saturated aqueous $NaHCO_3$. The organic layer was dried with Na_2SO_4, concentrated to a small volume, and chromatographed on silica gel column (Ø 2 × 30 cm), and the column was eluted with benzene/Et_2O/ethanol (15:5:1 v/v/v). The single red-purple band was collected and evaporated to dryness to yield 24.1 mg (22.1 mmol, 87%) of the products. The diastereomers were similarly separated by HPLC. The HPLC conditions were as follows; for resolution of meso and chiral **1**·Zn, YMC SH-043-5 (Ø 2.0 × 25 cm), benzene/THF (97:3 v/v) eluent at a flow rate of 7.0 mL/min, and for resolution of **1**(+)·Zn and **1**(−)·Zn, YMC A-K43 (Ø 2.0 × 25 cm), hexane/CH_2Cl_2/EtOH (70:30:2 v/v/v) eluent at a flow rate of 7.0 mL/min. The separation factor α and the resolution factor R_s for the chiral resolution were 1.12 and 1.53, respectively. UV−vis of **1**(+)·Zn λ_{max}, nm (log ε): 428 (5.46), 554 (4.16), 589 (3.51). CD spectra of **1**(±)·Zn in $CHCl_3$ (350−700 nm): 3.2×10^4 (428 nm), -1.9×10^4 (350 nm). CD of **1**(−)·Zn: -3.2×10^4 (428 nm), 1.9×10^4 (350 nm). ^{1}H NMR of **1**(−)·Zn (400 MHz, CD_2Cl_2): δ 9.24 (ABq, n_{AB} = 4.7 Hz, 2H, pyrrole), 9.23 (ABq, n_{AB} 4.7 Hz, 2H, pyrrole), 9.18 (s, 2H, pyrrole), 9.09 (s, 2H, pyrrole), 8.78 (d, J = 7.9 Hz, 2H), 8.69 (d, J = 8.4 Hz, 2H), 8.52 (d, J = 8.4 Hz, 2H), 8.50 (d, J = 7.9 Hz, 2H), 7.96 (ddd, J = 1.4, 8.4, 8.4 Hz, 2H), 7.94 (ddd, J = 1.4, 8.4, 8.4 Hz, 2H), 7.80 (ddd, J = 1.0, 7.9, 7.9 Hz, 2H), 7.77 (ddd, J = 1.0, 7.9, 7.9 Hz, 2H), 7.44 (d, J = 8.3 Hz, 2H, bridged benzene), 7.35 (d, J = 8.3 Hz, 2H, bridged benzene), 7.34 (bs, 2H, amide NH), 6.76 (bs, 2H, amide NH), 6.72 (s, 2H, bridged benzene). FABMS of *meso*-**1**·Zn: *m/z* 1087 (MH^+). FABMS of **1**(+)·Zn: *m/z* 1087 (MH^+). Anal. Calcd (*meso*-**1**·Zn) for $C_{60}H_{34}N_{10}O_8$-Zn: C, 66.21; H, 3.15; N, 12.87. Found: C, 65.82; H, 3.08; N, 13.07.

Preparation of 2·Zn. The porphyrin receptor, **2**, was prepared in THF and metalated by a method similar to that for **1**. ^{1}H NMR of **2**·Zn (500 MHz, $CDCl_3$): δ 9.28 (s, 4H, pyrrole), 9.12 (s, 4H, pyrrole), 8.78 (d, J = 7 Hz, 4H), 8.48 (d, J = 7 Hz, 4H), 7.90 (dd, J = 7, 7 Hz, 4H), 7.72 (dd, J = 7, 7 Hz, 4H), 7.43 (d, J = 8 Hz, 4H, bridged benzene), 7.37 (s, 4H, amide NH), 6.99 (dd, J = 8, 8 Hz, 2H, bridged benzene), 9.12 (s, 2H, bridged benzene). UV−vis (CH_2Cl_2) λ_{max}, nm (log ε): 429 (5.51), 555 (4.16), 590 (3.70). FABMS *m/z*: 997 (MH^+). Anal. Calcd for $C_{60}H_{36}N_8O_4Zn$: C, 72.18; H, 3.63; N, 11.22. Found: C, 72.29; H, 3.56; N, 11.47.

Preparation of 3. To a solution of α,α,β,β-T_{am}PP (21.2 mg, 0.031 mmol) in dry NMP (20 mL) was added 5-nitroisophthaloyl chloride (15.6 mg, 0.062 mmol) in an ice bath under a nitrogen atmosphere with stirring. After 12 h, the solvent was evaporated in vacuo (100 mmHg, 160 °C), $CHCl_3$ (50 mL) was added to the residue and the resulting dark purple powder was isolated by filtration. The product was washed two times with $CHCl_3$ to yield 0.0243 g of the desired product (0.0237 mmol, 76%). ^{1}H NMR of **3** (500 MHz, $CDCl_3$−CF_3CO_2D): δ 9.55 (s, 4H), 9.22 (s, 4H), 8.59 (d, J = 7.5 Hz,

(27) Ruggli, P.; Reichwein, H. *Helv. Chim. Acta* **1937**, *20*, 905.

(28) Greenstein, J. P.; Winitz, M. *Chemistry of Amino Acids*; Krieger Publishing Co.: Malabar, FL, 1984; pp 925−943.

4H), 8.24 (d, J = 7.5 Hz, 4H), 8.14 (dd, J = 7.5, 7.5 Hz, 4H), 8.07 (dd, J = 7.5, 7.5 Hz, 4H), 7.76 (s, 4H), 6.25 (s, 2H). FABMS: m/z 1025 (MH^+).

The Zn insertion of **3** was performed similarly by using $Zn(OAc)_2$ to give **3**·Zn in 35% yield. ^1H NMR (500 MHz, $CDCl_3$): δ 9.24 (s, 4H, pyrrole), 9.10 (s, 4H, pyrrole), 8.71 (d, J = 7.5 Hz, 4H), 8.48 (d, J = 7.5 Hz, 4H), 7.92 (dd, J = 7.5, 7.5 Hz, 4H), 7.76 (dd, J = 7.5, 7.5 Hz, 4H), 7.35 (s, 4H, bridged benzene), 6.25 (s, 2H, bridged benzene). UV−vis (CH_2Cl_2) λ_{max}, nm (log e): 429 (5.35), 556 (3.97) 588 (3.54). FABMS: m/z 1087 (MH^+). Anal. Calcd for $C_{60}H_{34}N_{10}O_8Zn$: C, 66.21; H, 3.15; N, 12.87. Found: C, 66.19; H, 3.28; N, 13.02.

Preparation of 4. The porphyrin receptor, **4**, was prepared in 77% yield and metalated in 48% yield by a method similar to that for **3**. ^1H NMR of **4** (500 MHz, $CDCl_3$−CF_3CO_2D): δ 9.47 (s, 1H, pyrrole), 9.44 (d, J = 3.5 Hz, 1H, pyrrole), 9.38 (d, J = 3.5 Hz, 1H, pyrrole), 9.36 (s, 1H, pyrrole), 9.24 (d, J = 3.5 Hz, 1H, pyrrole), 9.23 (d, J = 3.5 Hz, 1H, pyrrole), 9.19 (d, J = 3.5 Hz, 1H, pyrrole), 9.18 (d, J = 3.5 Hz, 1H, pyrrole), 8.59 (d, J = 7.5 Hz, 1H), 8.55 (d, J = 7.5 Hz, 1H), 8.52 (d, J = 7.5 Hz, 1H), 8.48 (d, J = 7.5 Hz, 1H), 8.34 (d, J = 7.5 Hz, 1H), 8.33 (d, J = 7.5 Hz, 1H), 8.21 (d, J = 7.5 Hz, 1H), 8.19 (d, J = 7.5 Hz, 1H), 8.12 (m, 4H), 8.02 (m, 4H), 7.46 (s, 2H), 5.83 (s, 2H). FABMS: m/z 1093 (M − 22). ^1H NMR of **4**·Zn (500 MHz, DMSO-d_6): δ 8.98 (s, 2H, amide NH), 8.95 (s, 2H, amide NH), 8.90 (d, J = 3.7 Hz, 2H, pyrrole), 8.89 (d, J = 3.7 Hz, 2H, pyrrole), 8.79 (d, J = 3.7 Hz, 2H, pyrrole), 8.77 (d, J = 3.7 Hz, 2H, pyrrole), 8.38 (d, J = 7.2 Hz, 2H), 8.37 (d, J = 7.2 Hz, 2H), 8.19 (d, J = 8.0 Hz, 2H), 8.15 (d, J = 8.0 Hz, 2H), 7.88 (dd, J = 7.5, 8.0 Hz, 4H), 7.78 (dd, J = 7.2, 7.5 Hz, 4H), 7.55 (s, 2H, bridged benzene), 6.18 (s, 2H, bridged benzene). UV−vis (CH_2Cl_2) λ_{max}, nm (log ϵ): 428 (5.46), 553 (4.15), 589 (3.52). FABMS: m/z 1155 (M-22). Anal. Calcd for $C_{60}H_{32}N_{12}O_{12}Zn$: C, 61.16; H, 2.74; N, 14.26. Found: C, 61.68; H, 2.55; N, 13.92.

JA951226I